

# Prompt $J/\psi$ plus photon associated electroproduction at DESY HERA

B.A. Kniehl<sup>1,a</sup>, C.P. Palisoc<sup>2</sup>

<sup>1</sup> II. Institut für Theoretische Physik, Universität Hamburg, Luruper Chaussee 149, 22761 Hamburg, Germany

<sup>2</sup> National Institute of Physics, University of the Philippines, Diliman, Quezon City 1101, Philippines

Received: 3 July 2006 /

Published online: 24 October 2006 – © Springer-Verlag / Società Italiana di Fisica 2006

**Abstract.** We study the production of a prompt  $J/\psi$  meson in association with a prompt photon in  $ep$  deep-inelastic scattering within the factorisation formalism of non-relativistic quantum chromodynamics (NRQCD) and demonstrate that this process provides a clean probe of the colour-octet mechanism at DESY HERA. Our analysis is based on an updated set of non-perturbative NRQCD matrix elements obtained through a joint fit to data on charmonium inclusive hadroproduction from runs I and II at the Fermilab Tevatron.

**PACS.** 12.38.-t; 12.38.Bx; 13.85.Fb; 14.40.Gx

## 1 Introduction

Since the discovery of the  $J/\psi$  meson in 1974, charmonium has provided a useful laboratory for quantitative tests of quantum chromodynamics (QCD) and, in particular, of the interplay of perturbative and non-perturbative phenomena. The factorisation formalism [1, 2] of non-relativistic QCD (NRQCD) [3] provides a rigorous theoretical framework for the description of heavy-quarkonium production and decay. This formalism implies a separation of short-distance coefficients, which can be calculated perturbatively as expansions in the strong-coupling constant  $\alpha_s$ , from long-distance matrix elements (MEs), which must be extracted from experiment. The relative importance of the latter can be estimated by means of velocity scaling rules; i.e., the MEs are predicted to scale with a definite power of the heavy-quark ( $Q$ ) velocity  $v$  in the limit  $v \ll 1$ . In this way, the theoretical predictions are organised as double expansions in  $\alpha_s$  and  $v$ . A crucial feature of this formalism is that it takes into account the complete structure of the  $Q\bar{Q}$  Fock space, which is spanned by the states  $n = {}^{2S+1}L_J^{(a)}$  with definite spin  $S$ , orbital angular momentum  $L$ , total angular momentum  $J$ , and colour multiplicity  $a = 1, 8$ . The hierarchy of the MEs predicted by the velocity scaling rules is explained for the  $J/\psi$ ,  $\psi'$ , and  $\chi_{cJ}$  mesons in Table 1. In particular, this formalism predicts the existence of colour-octet (CO) processes in nature. This means that  $Q\bar{Q}$  pairs are produced at short distances in CO states and subsequently evolve into physical, colour-singlet (CS) quarkonia by the non-perturbative

emission of soft gluons. In the limit  $v \rightarrow 0$ , the traditional CS model (CSM) [4–7] is recovered in the case of  $S$ -wave quarkonia. The greatest triumph of this formalism was that it was able to correctly describe [8–11] the cross section of inclusive charmonium hadroproduction measured in  $p\bar{p}$  collisions at the Fermilab Tevatron [12, 13], which had turned out to be more than one order of magnitude in excess of the theoretical prediction based on the CSM. Apart from this phenomenological drawback, the CSM also suffers from severe conceptual problems indicating that it is incomplete. These include the presence of logarithmic infrared singularities in the  $\mathcal{O}(\alpha_s)$  corrections to  $P$ -wave decays to light hadrons and in the relativistic corrections to  $S$ -wave annihilation [14], and the lack of a general argument for its validity in higher orders of perturbation theory.

In order to convincingly establish the phenomenological significance of the CO processes, it is indispensable to identify them in other kinds of high-energy experiments as well. Studies of charmonium production in  $ep$  photoproduction,  $ep$  and  $\nu N$  deep-inelastic scattering (DIS),  $e^+e^-$  annihilation in the continuum,  $Z$ -boson decays,  $\gamma\gamma$  collisions, and  $b$ -hadron decays may be found in the literature; for reviews, see [15–18]. Furthermore, the polarisation of  $\psi'$  mesons produced directly and of  $J/\psi$  mesons produced promptly, i.e., either directly or via the feed-down from heavier charmonia, which also provides a sensitive probe of CO processes, was investigated [19–21]. Until recently, none of these studies was able to prove or disprove the NRQCD factorisation hypothesis. However, H1 data of  $e + p \rightarrow e + J/\psi + X$  in DIS at the DESY Hadron Electron Ring Accelerator (HERA) [22–24] and DELPHI data of  $\gamma + \gamma \rightarrow J/\psi + X$  at the CERN Large Electron Positron Collider

<sup>a</sup> e-mail: kniehl@desy.de

**Table 1.** Values of  $k$  in  $\langle \mathcal{O}^H[n] \rangle \propto v^k$  for  $H = J/\psi, \psi', \chi_{cJ}$ 

$k$	$J/\psi, \psi'$	$\chi_{cJ}$
3	${}^3S_1^{(1)}$	–
5	–	${}^3P_J^{(1)}, {}^3S_1^{(8)}$
7	${}^1S_0^{(8)}, {}^3S_1^{(8)}, {}^3P_J^{(8)}$	–

(LEP2) [25] provide first independent evidence for it by agreeing with the respective NRQCD predictions [26–30].

In this paper, we identify the DIS process

$$e + p \rightarrow J/\psi + \gamma + X \quad (1)$$

as a clean probe of the CO mechanism and propose its experimental study at HERA II. In fact, among the partonic subprocesses contributing at LO,

$$e + \gamma \rightarrow e + c\bar{c} \left[ {}^3S_1^{(1)} \right] + \gamma, \quad (2)$$

$$e + g \rightarrow e + c\bar{c} \left[ {}^3S_1^{(8)} \right] + \gamma, \quad (3)$$

the latter is by far dominant because, in the relevant range of  $x$  and  $Q^2$ , the density of gluons in the proton is so much higher than the one of photons that the  $\mathcal{O}(v^4)$  suppression of  $\langle \mathcal{O}^{J/\psi} [{}^3S_1^{(8)}] \rangle$  relative to  $\langle \mathcal{O}^{J/\psi} [{}^3S_1^{(1)}] \rangle$  (see Table 1) is inconsequential. The emission of photons off the proton can happen either elastically or inelastically, i.e., the proton stays intact or is destroyed. In both cases, the parton density function (PDF) can be evaluated in the Weizsäcker–Williams approximation [31, 32]. Besides electromagnetic proton interaction, also diffractive scattering off the proton, via pomeron exchange, allows for CS processes. However, such events will be accumulated at the border of the phase space, at  $z \lesssim 1$ , where  $z$  is the inelasticity variable defined in Sect. 2. By the same token, they can be eliminated from the experimental data set by applying an appropriate acceptance cut on  $z$ . In this paper, we assume this to be done.

The potential of  $J/\psi$  plus photon associated production to probe the CO mechanism was already investigated for photoproduction in  $ep$  scattering [33]. In that case, however, the bulk of the cross section, more than 2/3 for  $J/\psi$  transverse momenta  $p_T > 1$  GeV (see Table II of [33]), is due to the CS channel  $g + g \rightarrow c\bar{c} [{}^3S_1^{(1)}] + \gamma$  in resolved photoproduction. Specifically, the photoproduction analogue of process (3),  $\gamma + g \rightarrow c\bar{c} [{}^3S_1^{(8)}] + \gamma$ , only makes up 1/5 of the total cross section [33]. On the other hand, the probability of a photon to appear resolved rapidly decreases with its size  $1/Q^2$ , so that the situation encountered in [33] is subject to a dramatic change as one passes from photoproduction to DIS.

In [34], prompt  $J/\psi$  plus photon associated photoproduction in  $\gamma\gamma$  collisions was studied in next-to-leading order (NLO), and sizeable corrections to the cross section were found. Since the present analysis is at an ex-

ploratory level, considering process (1) for the first time, we stay at LO. A NLO analysis of process (1) would be more involved than in the case of [34], due to the presence of  $Q^2$  as an additional mass scale, and is left for future work.

This paper is organised as follows. In Sect. 2, we collect the formulas from which the LO cross section of process (1) can be evaluated. In Sect. 3, we update the extraction of the NRQCD MEs of the  $J/\psi$ ,  $\psi'$ , and  $\chi_{cJ}$  mesons in [19] by including in the fit CDF data from Tevatron run II [35] besides that from run I [12, 13]. In Sect. 4, we then present our predictions for the cross section of process (1) under HERA II experimental conditions and demonstrate that this is an excellent probe of the CO mechanism. Our conclusions are contained in Sect. 5.

## 2 Analytic results

We now present our analytic results for the cross section of process (1). We work at LO in the parton model of QCD with  $n_f = 3$  active quark flavours and employ the NRQCD factorisation formalism [1, 2] to describe the formation of the  $J/\psi$  meson. We start by defining the kinematics. We denote the four-momenta of the incoming lepton and proton and the outgoing lepton,  $J/\psi$  meson, and photon by  $k$ ,  $P$ ,  $k'$ ,  $p_\psi$ , and  $p'$ , respectively. The parton  $a$  struck by the virtual photon ( $\gamma^*$ ) carries four-momentum  $p = xP$ . The virtual photon has four-momentum  $q = k - k'$ , and it is customary to define  $Q^2 = -q^2 > 0$ ,  $y = q \cdot P / k \cdot P$ , and  $z = p_\psi \cdot P / q \cdot P$ . In the proton rest frame,  $y$  and  $z$  measure the relative lepton energy loss and the fraction of the virtual-photon energy transferred to the  $J/\psi$  meson, respectively. We neglect the masses of the proton, lepton, and light quarks, call the one of the  $J/\psi$  meson  $M_\psi$ , and take the charm-quark mass to be  $m_c = M_\psi/2$ . In our approximation, the proton remnant  $X$  has zero invariant mass,  $M_X^2 = (P - p)^2 = 0$ . The centre-of-mass (CM) energy squares of the  $ep$  and  $\gamma^*p$  collision are  $S = (k + P)^2$  and  $W^2 = (q + P)^2 = yS - Q^2$ , respectively. As usual, we define the partonic Mandelstam variables as  $s = (q + p)^2 = xyS - Q^2$ ,  $t = (q - p_\psi)^2 = -xy(1 - z)S$ , and  $u = (p - p_\psi)^2 = M_\psi^2 - xyzS$ . By four-momentum conservation, we have  $s + t + u = M_\psi^2 - Q^2$ . In the  $\gamma^*p$  CM frame, the  $J/\psi$  meson has transverse momentum and rapidity

$$p_T^* = \frac{\sqrt{t(su + Q^2 M_\psi^2)}}{s + Q^2}, \quad (4)$$

$$y_\psi^* = \frac{1}{2} \ln \frac{s(M_\psi^2 - u)}{s(M_\psi^2 - t) + Q^2 M_\psi^2} + \frac{1}{2} \ln \frac{W^2}{s}, \quad (5)$$

respectively. Here and in the following, we denote the quantities referring to the  $\gamma^*p$  CM frame by an asterisk. The second term on the right-hand side of (5) originates from the Lorentz boost from the  $\gamma^*a$  CM frame to the  $\gamma^*p$  one. Here,  $y_\psi^*$  is taken to be positive in the direction of the

three-momentum of the virtual photon, in accordance with HERA conventions [22–24].

The cross sections of processes (2) and (3) may be conveniently calculated by applying the covariant-projector method of [36]. They are related to the one of  $e + g \rightarrow e + c\bar{c} [{}^3S_1^{(8)}] + g$ , given in (13) of [26], by

$$\begin{aligned} & \frac{d^3\sigma}{dy dQ^2 dt} \left( e + \gamma \rightarrow e + c\bar{c} [{}^3S_1^{(1)}] + \gamma \right) \\ &= \frac{64 \alpha^2}{9 \alpha_s^2} \frac{d^3\sigma}{dy dQ^2 dt} \left( e + g \rightarrow e + c\bar{c} [{}^3S_1^{(1)}] + g \right), \\ & \frac{d^3\sigma}{dy dQ^2 dt} \left( e + g \rightarrow e + c\bar{c} [{}^3S_1^{(8)}] + \gamma \right) \\ &= 2 \frac{\alpha}{\alpha_s} \frac{d^3\sigma}{dy dQ^2 dt} \left( e + g \rightarrow e + c\bar{c} [{}^3S_1^{(1)}] + g \right), \end{aligned} \quad (6)$$

where the proportionality factors account for colour and coupling adjustments.

According to the factorisation theorems of the parton model and NRQCD, the cross section of process (1) is then evaluated as

$$\begin{aligned} & \frac{d^2\sigma}{dy dQ^2} (e + p \rightarrow e + J/\psi + \gamma + X) \\ &= \int_{(Q^2 + M_\psi^2)/(yS)}^1 dx \int_{-(s+Q^2)/(s-M_\psi^2)/s}^0 dt \\ & \quad \times \sum_a f_{a/p}(x, M) \sum_n \langle \mathcal{O}^{J/\psi}[n] \rangle \\ & \quad \times \frac{d^3\sigma}{dy dQ^2 dt} (e + a \rightarrow e + c\bar{c}[n] + \gamma), \end{aligned} \quad (7)$$

where the sums run over  $(a, n) = (\gamma, {}^3S_1^{(1)}), (g, {}^3S_1^{(8)})$ ,  $f_{a/p}(x, M)$  is the PDF of parton  $a$  in the proton at factori-

sation scale  $M$ , and  $(d^3\sigma/dy dQ^2 dt) (e + a \rightarrow e + c\bar{c}[n] + \gamma)$  are given by (6). The kinematically allowed ranges of  $y$  and  $Q^2$  are  $M_\psi^2/S < y < 1$  and  $0 < Q^2 < yS - M_\psi^2$ , respectively.

Prompt  $J/\psi$  production may be conveniently described by inserting in (7) the effective MEs specified in (20) of [34].

### 3 Determination of the MEs

The recent CDF measurement of prompt  $J/\psi$  inclusive hadroproduction in run II at the Tevatron (with  $\sqrt{S} = 1.96$  TeV and  $|y_\psi| < 0.6$ ) [35] allows us to update and improve our knowledge of the CO MEs. Previous determinations by one of us in collaboration with Kramer [37, 38] and with Braaten and Lee [19] were only based on run I data (with  $\sqrt{S} = 1.8$  TeV and  $|y_\psi| < 0.6$ ) [12, 13]. However, the latter data were more detailed because the prompt  $J/\psi$  sample was explicitly broken down into direct  $J/\psi$  mesons, feed-down from  $\psi'$  mesons, and feed-down from  $\chi_{cJ}$  mesons. In order to make maximum use of the available information, we perform a joint fit to the data from runs I and II, which otherwise proceeds along the lines of [19]. First, the CS MEs  $\langle \mathcal{O}^{\psi(nS)} [{}^3S_1^{(1)}] \rangle$ , with  $n = 1, 2$ , and  $\langle \mathcal{O}^{\chi_{c0}} [{}^3P_0^{(1)}] \rangle$  are extracted from the measured partial decay widths of  $\psi(nS) \rightarrow l^+ + l^-$  and  $\chi_{c2} \rightarrow \gamma + \gamma$  [39], respectively. Then, the CO MEs  $\langle \mathcal{O}^{\psi(nS)} [{}^3S_1^{(8)}] \rangle$ ,  $\langle \mathcal{O}^{\psi(nS)} [{}^1S_0^{(8)}] \rangle$ ,  $\langle \mathcal{O}^{\psi(nS)} [{}^3P_0^{(8)}] \rangle$ , and  $\langle \mathcal{O}^{\chi_{c0}} [{}^3S_1^{(8)}] \rangle$  are fitted to the  $p_T$  distributions of  $\psi(nS)$  and  $\chi_{cJ}$  inclusive hadroproduction [12, 13, 35] and the cross-section ratio  $\sigma_{\chi_{c2}}/\sigma_{\chi_{c1}}$  [40] measured at the Tevatron. In contrast to the run I data [12, 13], the run II data [35] reach down to  $p_T = 0$ . It turns out that the run II data in the newly covered low- $p_T$  range are comparable to or below the CSM prediction, so that their inclusion would spoil

**Table 2.** NRQCD MEs of the  $J/\psi$ ,  $\psi'$ , and  $\chi_{cJ}$  mesons obtained as described in the text using the MRST2001LO [41] and CTEQ6L1 [42] PDFs. The errors are experimental only

	MRST2001LO [41]	CTEQ6L1 [42]
$\langle \mathcal{O}^{J/\psi} [{}^3S_1^{(1)}] \rangle$	$1.5 \pm 0.1 \text{ GeV}^3$	$1.4 \pm 0.1 \text{ GeV}^3$
$\langle \mathcal{O}^{J/\psi} [{}^3S_1^{(8)}] \rangle$	$(3.9 \pm 1.4) \times 10^{-4} \text{ GeV}^3$	$(2.3 \pm 0.2) \times 10^{-3} \text{ GeV}^3$
$M_{3.7,3.6}^{J/\psi}$	$(6.0 \pm 0.1) \times 10^{-2} \text{ GeV}^3$	$(7.3 \pm 0.2) \times 10^{-2} \text{ GeV}^3$
$\langle \mathcal{O}^{\psi'} [{}^3S_1^{(1)}] \rangle$	$(6.7 \pm 0.5) \times 10^{-1} \text{ GeV}^3$	$(6.7 \pm 0.5) \times 10^{-1} \text{ GeV}^3$
$\langle \mathcal{O}^{\psi'} [{}^3S_1^{(8)}] \rangle$	$(8.8 \pm 1.2) \times 10^{-4} \text{ GeV}^3$	$(2.0 \pm 0.2) \times 10^{-3} \text{ GeV}^3$
$M_{3.5}^{\psi'}$	$(1.1 \pm 0.1) \times 10^{-2} \text{ GeV}^3$	$(1.0 \pm 0.2) \times 10^{-2} \text{ GeV}^3$
$\langle \mathcal{O}^{\chi_{c0}} [{}^3P_0^{(1)}] \rangle$	$(1.2 \pm 0.1) \times 10^{-1} \text{ GeV}^5$	$(1.2 \pm 0.1) \times 10^{-1} \text{ GeV}^5$
$\langle \mathcal{O}^{\chi_{c0}} [{}^3S_1^{(8)}] \rangle$	$(4.7 \pm 0.6) \times 10^{-4} \text{ GeV}^3$	$(1.1 \pm 0.1) \times 10^{-3} \text{ GeV}^3$

the fit. Therefore, we only include the 14 data points with  $p_T > 4.25$  GeV. Since the fit results for  $\langle \mathcal{O}^{\psi(nS)} [^1S_0^{(8)}] \rangle$  and  $\langle \mathcal{O}^{\psi(nS)} [^3P_0^{(8)}] \rangle$  are strongly correlated, we consider the linear combination

$$M_r^{\psi(nS)} = \langle \mathcal{O}^{\psi(nS)} [^1S_0^{(8)}] \rangle + \frac{r}{m_c^2} \langle \mathcal{O}^{\psi(nS)} [^3P_0^{(8)}] \rangle, \quad (8)$$

where the value of  $r$  is chosen so that the error on  $M_r^{\psi(nS)}$  is minimised. The minimisation in  $\chi^2$  is performed exactly, by solving a set of seven linear equations for the seven unknown CO MEs.

The relevant partonic cross sections may be found in [10,11]. We take the charm-quark mass to be  $m_c = (1.5 \pm 0.1)$  GeV and adopt the relevant feed-down and leptonic decay branching fractions from [39]. As for the proton PDFs, we use the latest LO sets by Martin, Roberts, Stirling, and Thorne (MRST2001LO) [41] and the Co-

ordinated Theoretical-Experimental Project on QCD (CTEQ6L1) [42]. For consistency, we employ the one-loop formula for  $\alpha_s^{(3)}(\mu)$  and choose the asymptotic scale parameter to be  $\Lambda_{\text{QCD}}^{(3)} = 253$  MeV (246 MeV), appropriate for the MRST2001LO (CTEQ6L1) PDFs. We identify the renormalisation scale  $\mu$  and the factorisation scale  $M$  with the charmonium transverse mass  $m_T = \sqrt{p_T^2 + M_\psi^2}$ .

The sets of MEs thus obtained with the MRST2001LO and CTEQ6L1 PDFs are summarised in Table 2. The respective values of  $\chi^2$  per degree of freedom are 49/52 and 50/52. The quoted errors are of experimental origin only. Comparing Table 2 with Table I of [19], where previous MRST and CTEQ PDFs were used, we observe that the MEs obtained with CTEQ PDFs are only moderately changed. On the other hand, the MRST values of  $\langle \mathcal{O}^{\psi(nS)} [^3S_1^{(8)}] \rangle$  and  $\langle \mathcal{O}^{\chi_{c0}} [^3S_1^{(8)}] \rangle$  in Table 2 are appreciably smaller than in [19].

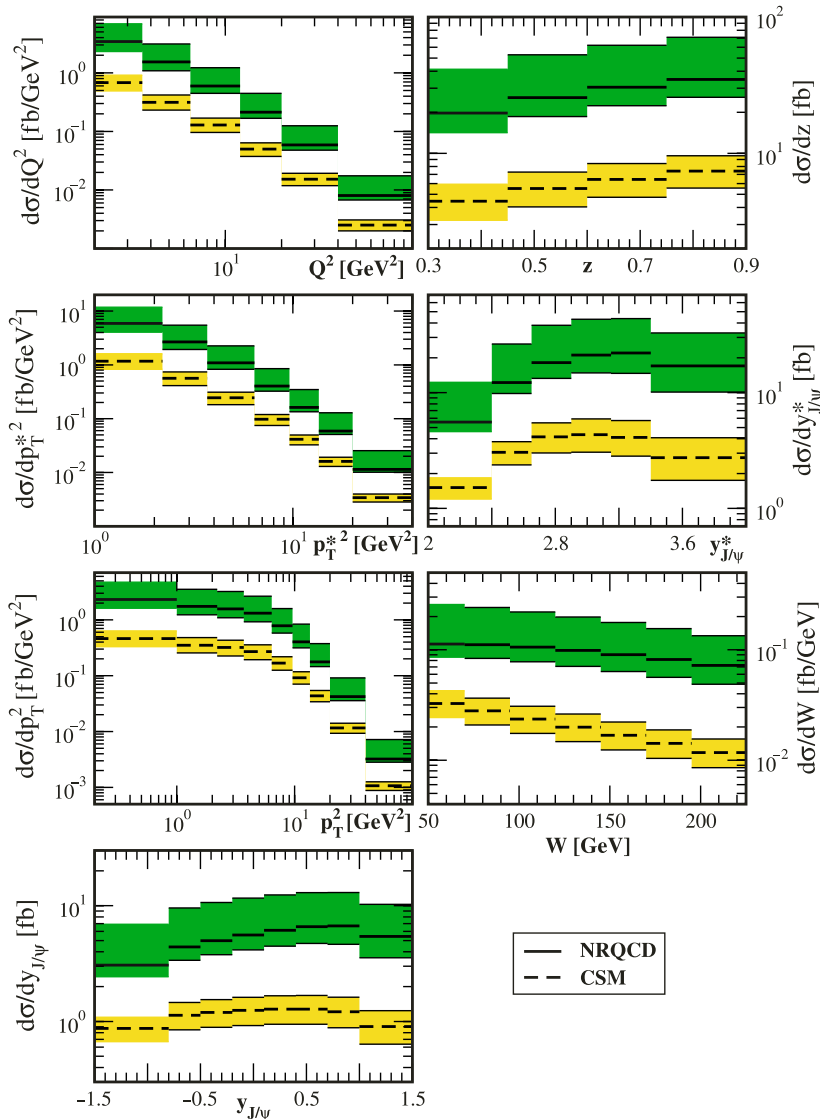


**Fig. 1.** NRQCD (solid lines) and CSM (dashed lines) predictions of the  $Q^2$ ,  $z$ ,  $p_T^{*2}$ ,  $y_\psi^*$ ,  $p_T^2$ ,  $W$ , and  $y_\psi$  distributions of prompt  $J/\psi$  plus photon associated electroproduction at HERA II in the kinematic region defined by  $2 < Q^2 < 100$  GeV,  $50 < W < 225$  GeV,  $0.3 < z < 0.9$ , and  $p_T^{*2} > 1$  GeV<sup>2</sup>. The shaded bands indicate the theoretical uncertainty

## 4 Prompt $J/\psi$ plus photon associated electroproduction

We are now in a position to present our theoretical predictions for the cross section of process (1) under HERA II experimental conditions. They are evaluated from the formulas listed in Sect. 2 with the inputs and conventions described in Sect. 3, except that we now set  $\mu = M = \xi \sqrt{Q^2 + M_\psi^2}$  and vary the scale parameter  $\xi$  between 1/2 and 2 about the default value 1. Since (7) is sensitive to a linear combination of  $\langle \mathcal{O}^{\psi(nS)} [^1S_0^{(8)}] \rangle$  and  $\langle \mathcal{O}^{\psi(nS)} [^3P_0^{(8)}] \rangle$  different from the one appearing in (8), we write

$$\begin{aligned} \langle \mathcal{O}^{\psi(nS)} [^1S_0^{(8)}] \rangle &= \kappa M_r^{\psi(nS)}, \\ \langle \mathcal{O}^{\psi(nS)} [^3P_0^{(8)}] \rangle &= (1 - \kappa) \frac{m_c^2}{r} M_r^{\psi(nS)}; \end{aligned} \quad (9)$$

and vary  $\kappa$  between 0 and 1 about the default value 1/2.

In order to estimate the theoretical uncertainties in our predictions, we vary the unphysical parameters  $\xi$  and  $\kappa$  as indicated above, take into account the experimental errors on  $m_c$  and the default MEs, and switch from the MRST2001LO PDFs [41], which we take as our default, to the CTEQ6L1 ones [42], properly adjusting  $\Lambda_{\text{QCD}}^{(3)}$  and the MEs. We then combine the individual shifts in quadrature, allowing for the upper and lower half errors to be different.

In the laboratory frame of HERA II, electrons or positrons with energy  $E_e = 27.5$  GeV collide on protons with energy  $E_p = 920$  GeV, yielding a CM energy of  $\sqrt{S} = 2\sqrt{E_e E_p} = 318$  GeV. For definiteness, we adopt the experimental acceptance cuts from the recent H1 analysis of inclusive  $J/\psi$  electroproduction [23], which include  $2 < Q^2 < 100$  GeV,  $50 < W < 225$  GeV,  $0.3 < z < 0.9$ , and  $p_T^{*2} > 1$  GeV<sup>2</sup>. We consider cross-section distributions in  $Q^2$ ,  $W$ ,  $z$ ,  $p_T^{*2}$ ,  $y_\psi^*$ ,  $p_T^2$ , and  $y_\psi$ , where the last four variables refer to the  $J/\psi$  meson, adopting the binning from [23].

Our results are displayed in Fig. 1, where the NRQCD predictions (solid lines) are compared with the CSM ones (dashed lines). In each case, the theoretical uncertainties are indicated by the shaded bands. As expected from our discussion in Sect. 1, the NRQCD predictions vastly exceed the CSM ones, by almost one order of magnitude. The gaps are considerably larger than the theoretical errors. On the other hand, the shapes of the various cross-section distributions come out very similar in both approaches, which may be understood by observing that the partonic cross sections of the CS and CO channels in (6) are proportional to each other. From Fig. 1, we read off that the integrated NRQCD cross section is of order 10 fb. Given that the integrated luminosity to be collected by the end of HERA operation amounts to about 1 fb<sup>-1</sup>, one thus expects about 10 signal events.

## 5 Conclusions

We studied the electroproduction of prompt  $J/\psi$  mesons in association with prompt photons in  $ep$  collisions under

HERA II kinematic conditions to LO in the NRQCD [3] factorisation formalism [1, 2]. We considered cross-section distributions in all variables of current interest [22–24], including  $Q^2$ ,  $W$ ,  $z$ ,  $p_T^{*2}$ ,  $y_\psi^*$ ,  $p_T^2$ , and  $y_\psi$ . As input for our calculation, we used updated information on the NRQCD MEs extracted from a combined fit to data on inclusive charmonium hadroproduction collected by the CDF collaboration in runs I [12, 13] and II [35] at the Tevatron.

As a result of our study, we could identify prompt  $J/\psi$  plus photon associated electroproduction as a useful probe of the CO mechanism. In fact the NRQCD predictions turned out to exceed the CSM ones by almost one order of magnitude. Unfortunately, the cross-section distributions in both theories have very similar shapes, so that the NRQCD to CSM ratio cannot be further enhanced by specific acceptance cuts. Should this production process be experimentally observed with the rate predicted by NRQCD, then this would provide strong evidence in favour of the existence of CO processes in nature. In view of the moderate integrated cross section of order 10 fb, this is a challenging endeavour. This is an example of a study that would benefit from the extension of HERA operation beyond the summer of 2007.

*Acknowledgements.* The research of B.A.K. was supported in part by the BMBF through Grant No. 05 HT6GUA and the DFG through Grant No. KN 365/6-1. The research of C.P.P. was supported in part by the DFG through Graduiertenkolleg No. GRK 602/2 and by the Office of the Vice President for Academic Affairs of the University of the Philippines.

## References

1. G.T. Bodwin, E. Braaten, G.P. Lepage, Phys. Rev. D **51**, 1125 (1995)
2. G.T. Bodwin, E. Braaten, G.P. Lepage, Phys. Rev. D **55**, 5853(E) (1997)
3. W.E. Caswell, G.P. Lepage, Phys. Lett. B **167**, 437 (1986)
4. V.G. Kartvelishvili, A.K. Likhoded, S.R. Slabospitskiĭ, Yad. Fiz. **28**, 1315 (1978)
5. V.G. Kartvelishvili, A.K. Likhoded, S.R. Slabospitskiĭ, Sov. J. Nucl. Phys. **28**, 678 (1978)
6. E.L. Berger, D. Jones, Phys. Rev. D **23**, 1521 (1981)
7. R. Baier, R. Rückl, Phys. Lett. B **102**, 364 (1981)
8. E. Braaten, S. Fleming, Phys. Rev. Lett. **74**, 3327 (1995)
9. E. Braaten, T.C. Yuan, Phys. Rev. D **52**, 6627 (1995)
10. P. Cho, A.K. Leibovich, Phys. Rev. D **53**, 150 (1996)
11. P. Cho, A.K. Leibovich, Phys. Rev. D **53**, 6203 (1996)
12. CDF Collaboration, F. Abe et al., Phys. Rev. Lett. **79**, 572 (1997)
13. CDF Collaboration, F. Abe et al., Phys. Rev. Lett. **79**, 578 (1997)
14. R. Barbieri, R. Gatto, E. Remiddi, Phys. Lett. B **61**, 465 (1976)
15. E. Braaten, S. Fleming, T.C. Yuan, Ann. Rev. Nucl. Part. Sci. **46**, 197 (1996)
16. B.A. Kniehl, G. Kramer, Phys. Lett. B **413**, 416 (1997)
17. M. Krämer, Prog. Part. Nucl. Phys. **47**, 14 (2001)
18. M. Klasen, Rev. Mod. Phys. **74**, 1221 (2002)

19. E. Braaten, B.A. Kniehl, J. Lee, Phys. Rev. D **62**, 094005 (2000)
20. B.A. Kniehl, J. Lee, Phys. Rev. D **62**, 114027 (2000)
21. B.A. Kniehl, G. Kramer, C.P. Palisoc, Phys. Rev. D **68**, 114002 (2003)
22. H1 Collaboration, C. Adloff et al., Eur. Phys. J. C **10**, 373 (1999)
23. H1 Collaboration, C. Adloff et al., Eur. Phys. J. C **25**, 41 (2002)
24. ZEUS Collaboration, S. Chekanov et al., Eur. Phys. J. C **44**, 13 (2005)
25. DELPHI Collaboration, J. Abdallah et al., Phys. Lett. B **565**, 76 (2003)
26. B.A. Kniehl, L. Zwirner, Nucl. Phys. B **621**, 337 (2002)
27. B.A. Kniehl, L. Zwirner, Nucl. Phys. B **637**, 311 (2002)
28. B.A. Kniehl, L. Zwirner, Nucl. Phys. B **678**, 258 (2004)
29. M. Klasen, B.A. Kniehl, L.N. Mihaila, M. Steinhauser, Phys. Rev. Lett. **89**, 032001 (2002)
30. R.M. Godbole, D. Indumathi, M. Krämer, Phys. Rev. D **65**, 074003 (2002)
31. B.A. Kniehl, Phys. Lett. B **254**, 267 (1991)
32. M. Glück, M. Stratmann, W. Vogelsang, Phys. Lett. B **343**, 399 (1997)
33. M. Cacciari, M. Greco, M. Krämer, Phys. Rev. D **55**, 7126 (1997)
34. M. Klasen, B.A. Kniehl, L.N. Mihaila, M. Steinhauser, Phys. Rev. D **71**, 014016 (2005)
35. CDF Collaboration, D. Acosta et al., Phys. Rev. D **71**, 032001 (2005)
36. A. Petrelli, M. Cacciari, M. Greco, F. Maltoni, M.L. Mangano, Nucl. Phys. B **514**, 245 (1998)
37. B.A. Kniehl, G. Kramer, Eur. Phys. J. C **6**, 493 (1999)
38. B.A. Kniehl, G. Kramer, Phys. Rev. D **60**, 014006 (1999)
39. Particle Data Group, S. Eidelman et al., Phys. Lett. B **592**, 1 (2004)
40. CDF Collaboration, T. Affolder et al., Phys. Rev. Lett. **86**, 3963 (2001)
41. A.D. Martin, R.G. Roberts, W.J. Stirling, R.S. Thorne, Phys. Lett. B **531**, 216 (2002)
42. J. Pumplin, D.R. Stump, J. Huston, H.-L. Lai, P. Nadolsky, W.-K. Tung, JHEP **0207**, 012 (2002)